

# CONESCAPANHONDURAS2025paper125.pdf

 Institute of Electrical and Electronics Engineers (IEEE)

---

## Document Details

### Submission ID

trn:oid:::14348:477742410

### Submission Date

Jul 31, 2025, 10:22 PM CST

### Download Date

Aug 12, 2025, 6:27 PM CST

### File Name

CONESCAPANHONDURAS2025paper125.pdf

### File Size

3.8 MB

6 Pages





2,895 Words

15,015 Characters




# 9% Overall Similarity

The combined total of all matches, including overlapping sources, for each database.

## Match Groups

-  **18 Not Cited or Quoted 8%**  
Matches with neither in-text citation nor quotation marks
-  **3 Missing Quotations 1%**  
Matches that are still very similar to source material
-  **1 Missing Citation 0%**  
Matches that have quotation marks, but no in-text citation
-  **0 Cited and Quoted 0%**  
Matches with in-text citation present, but no quotation marks

## Top Sources

- 9%  Internet sources
- 5%  Publications
- 0%  Submitted works (Student Papers)

## Integrity Flags





### 0 Integrity Flags for Review

No suspicious text manipulations found.




Our system's algorithms look deeply at a document for any inconsistencies that would set it apart from a normal submission. If we notice something strange, we flag it for you to review.

A Flag is not necessarily an indicator of a problem. However, we'd recommend you focus your attention there for further review.

## Match Groups

-  **18 Not Cited or Quoted** 8%  
Matches with neither in-text citation nor quotation marks
-  **3 Missing Quotations** 1%  
Matches that are still very similar to source material
-  **1 Missing Citation** 0%  
Matches that have quotation marks, but no in-text citation
-  **0 Cited and Quoted** 0%  
Matches with in-text citation present, but no quotation marks

## Top Sources

- 9%  Internet sources
- 5%  Publications
- 0%  Submitted works (Student Papers)

## Top Sources

The sources with the highest number of matches within the submission. Overlapping sources will not be displayed.

1	Internet	dspace.ucuenca.edu.ec	1%
2	Internet	ore.exeter.ac.uk	<1%
3	Internet	fdocuments.in	<1%
4	Internet	www.vladimirgbic.com	<1%
5	Internet	repositorio.iica.int	<1%
6	Internet	nova_scientia.delasalle.edu.mx	<1%
7	Internet	pass.health.gov.bz	<1%
8	Internet	ksp.etri.re.kr	<1%
9	Internet	latamt.ieeer9.org	<1%
10	Internet	www.mdpi.com	<1%

11	Internet	monolith.asee.org	<1%
12	Internet	www.slideshare.net	<1%
13	Internet	revista.saludcyt.ar	<1%
14	Publication	Danish Iqbal, Barbora Buhnova. "Model-based Approach for Building Trust in Aut...	<1%
15	Publication	Kushmanda Saurav, Debdeep Sarkar, Kumar Vaibhav Srivastava. "CRLH Unit-Cell ...	<1%
16	Internet	revistas.ucc.edu.co	<1%
17	Internet	www.olade.org.ec	<1%
18	Publication	Nestor Zamora Cedeno, Orlando Philco Asqui, Emily Estupinan Chaw. "The perfor...	<1%

# Electronic Sea Level Sensor Prototype Using Moore Machines and RLC Circuit Modeling

**Abstract**—The equivalent circuit is a fundamental technique for modeling wave energy conversion systems with high accuracy in energy absorption. Given the constant progress in the design of these systems, it is essential to have a clear guide to develop an equivalent RLC model that not only ensures accuracy and proper operation, but also facilitates its adaptation to various research contexts. This paper proposes a methodology oriented to force analysis, incorporating a prototype sea level gauge, and details the construction of nonlinear circuit models capable of faithfully representing the dynamics of real systems. Inspired by the PowerBuoy approach, which uses vertical displacement of permanent magnets within a copper coil to harness wave motion, an improvement is introduced based on replacing air-core coils with ferrite-core coils, displacing the latter among several coils. This modification alters the inductive and reactive nature of the system, allowing the wave height to be measured and calculated more accurately.

**Index Terms**—Magnetic Sensors, microcontrollers, prototypes, resonant circuits, RLC circuits, state machine control.

## I. INTRODUCTION

Global dependence on petroleum derivatives as a primary source for electricity generation has generated serious environmental consequences, such as climate change and atmospheric pollution [1]. Faced with this scenario, the scientific community has focused its efforts on the development of sustainable alternatives, where renewable energy sources have acquired a fundamental role [2]. Honduras, due to its geographical location, has two extensive coastal areas with favorable conditions for the use of marine energy. In particular, wave energy - obtained from the movement of waves - represents a viable opportunity to diversify the national energy matrix [3], [4]. Despite its potential, this non-conventional renewable source has been scarcely explored in Central America, so its implementation would position Honduras as one of the pioneering countries in the region [5].

One of the main limitations identified in this research was the lack of access to local technical data from an operating wave power plant, which hindered the direct collection of information and the analysis of technical feasibility [6], [7]. In view of this situation, the design and development of a scaled prototype to simulate the behavior of a wave power system under controlled conditions was chosen [8], [9]. This experimental approach allowed addressing the central research question: how to design a device capable of calculating the wave height from its vertical motion? To answer this question, the development of an electronic device with the ability to accurately measure the sea level, using the principle of wave-induced displacement, was proposed.

## II. THEORETICAL FRAMEWORK

### A. Resonant Circuits

Resonance in a parallel circuit occurs when the capacitive reactance and inductive reactance are equal in magnitude but opposite in sign. In this condition, the total current reaches a minimum and the circuit impedance is at a maximum, allowing the voltage to remain constant and minimizing power losses [10]. This principle is widely used in radio frequency systems, telecommunications, and in the manufacture of filters for audio and video signals [11].

The resonant frequency in an RLC circuit is calculated with the expression:

$$f = \frac{1}{2\pi\sqrt{LC}} \quad (1)$$

where  $L$  is the inductance and  $C$  is the capacitance of the circuit. At this frequency, the maximum energy exchange between the reactive components occurs [10].

The operation of these circuits is based on the ability of the capacitor to store electrical energy and the coil to store magnetic energy. The energy oscillates between both elements until the excitation of the system ceases [11].

### B. Capacitive Reactance

The capacitive reactance represents the opposition of a capacitor to the passage of alternating current. Its value depends on the frequency of the signal and is determined by:

$$X_C = \frac{1}{2\pi fC} \quad (2)$$

where  $f$  is the operating frequency and  $C$  the capacitance. At higher frequencies, the capacitive reactance decreases, allowing higher current to pass.

### C. Inductance

Inductance is the property of a coil to induce an electromotive force (fem) when there is a variation in the current passing through it. It is calculated as:

$$L = \frac{N^2 \mu A}{l} \quad (3)$$

where  $N$  is the number of turns,  $\mu$  the core permeability,  $A$  the cross-sectional area and  $l$  the length of the solenoid [12]. In this work, the effect of changing the core (air vs. ferrite) on the inductance is explored, which allows the circuit characteristics to be modified in a controlled manner.

#### D. Inductive Reactance

The inductive reactance is the opposition of a coil to the passage of alternating current, and its value increases with frequency. It is expressed as:

$$X_L = 2\pi fL \quad (4)$$

This behavior is explained by Lenz's Law, which states that an inductor tends to oppose changes in the current passing through it [13]. By using cores of different magnetic permeabilities (such as air and ferrite), it is possible to modify the value of  $L$  and, therefore, the total reactance of the circuit.

#### E. Materials and Equipment

The following materials and equipment were used for the experimental setup:

- ATmega microcontroller.
- Resistors: three 100  $\Omega$  and three 220  $\Omega$  resistors connected in parallel, resulting in an equivalent resistance of approximately 68.25  $\Omega$ .
- Home-made air-core inductors.
- 470  $\mu\text{F}$  electrolytic capacitors.
- Ferrite core.
- Universal perforated bakelite board.
- Rigol DS1102E digital oscilloscope, 100 MHz.

These materials and equipment enabled the construction of a test system that simulates the behavior of a resonant circuit with variable inductance, allowing the analysis of how changes in core permeability affect key electrical variables.

### III. METHODOLOGY

#### A. Prototype of a coil

To initiate the experimental phase of the study, a prototype RLC circuit was built consisting of a resistor, a capacitor, and a copper coil with an air core. This basic configuration allows us to establish an initial reference without the influence of ferromagnetic materials, thus facilitating comparison with other variants. The air core was selected for its electromagnetic neutrality, which allowed the natural behavior of the inductance inside the circuit to be observed. Measurements were performed by connecting the node of interest to the ATmega micro controller via the analog input A0, allowing to record voltage variations as a function of the core configuration. This stage also served to verify the ADC response of the micro controller and laid the groundwork for further testing with ferrite cores. The data obtained were visualized with an oscilloscope, where the inductive effects of the system were clearly identified. The equivalent circuit diagram of the RLC-01 is shown in Fig. 1 [14]. The RLC-01 prototype with an air-core coil is depicted in Fig. 2 [14], while the prototype with a ferrite-core coil is presented in Fig. 3 [14].

The results obtained using the oscilloscope show an increase in the voltage at the node located between the equivalent resistance  $R_T$  and the parallel circuit formed by the capacitor and the coil ( $C-L$ ), as illustrated in Fig. 4 [14] and Fig. 5 [14]. This behavior confirms that the presence of a ferrite core alters

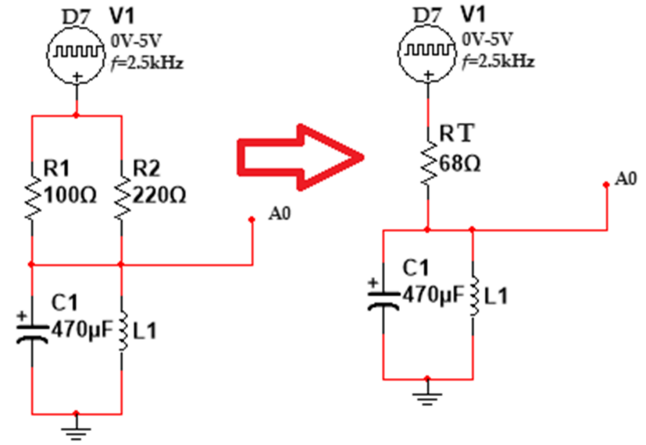


Fig. 1. Equivalent circuit of the RLC-01 prototype.

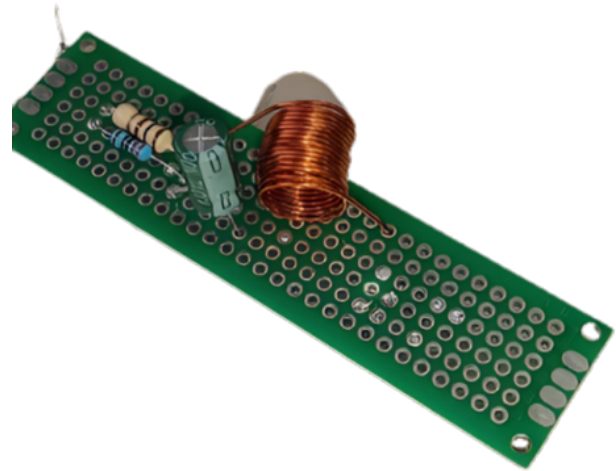


Fig. 2. RLC-01 prototype with air core coil.

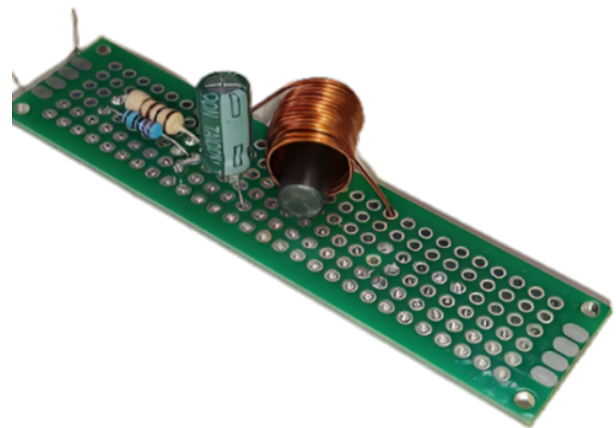


Fig. 3. RLC-01 prototype with ferrite core in the coil.

the reactance of the coil, resulting in a higher voltage observed at that point.

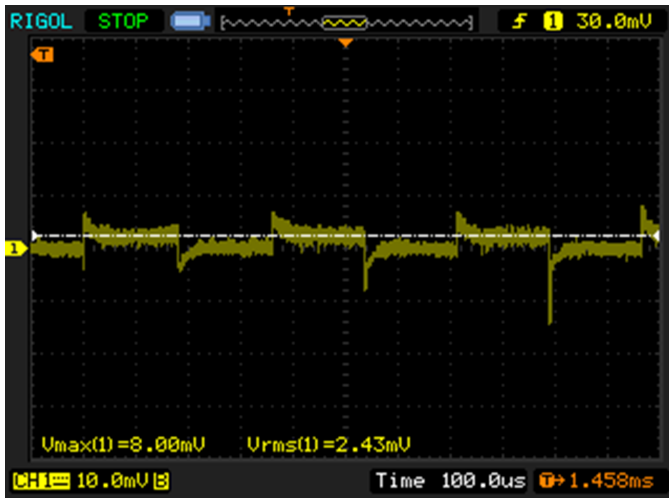


Fig. 4. Voltage with the inclusion of the air core.

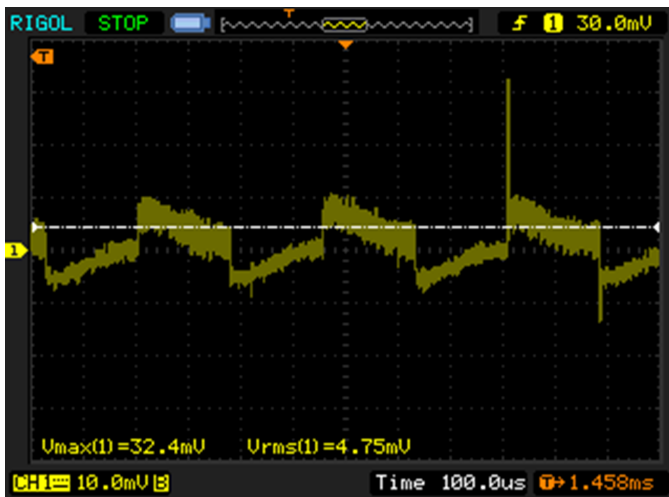


Fig. 5. Voltage with ferrite core inclusion.

Based on this potential variation, it was decided to connect the measurement node to the analog input A0 of the ATmega microcontroller as shown in Fig.6 [14], in order to determine if the voltage difference was significant enough to be detected by the analog-to-digital converter (ADC). To this end, comparative tests were performed with and without the ferrite inserted inside the coil.

Table I presents the digital readings obtained through the ADC at pin A0, corresponding to the RLC-01 prototype, under both experimental conditions.

The results obtained by reading bits from the ADC on the analog input A0 of the ATmega microcontroller were satisfactory, since they allowed digital detection of the potential change generated by the presence of a ferrite core in the coil. From these readings, a threshold value was established that facilitates rapid identification of the state of the coil, i.e.,

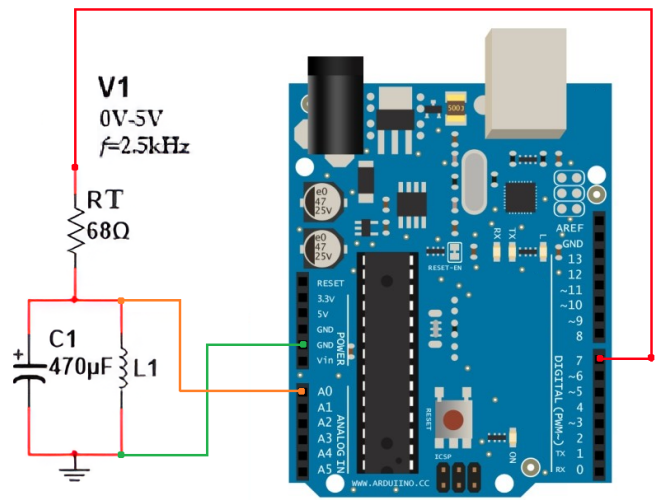


Fig. 6. Assembly of prototype RLC-01.

TABLE I  
VOLTAGE READINGS WITH AND WITHOUT FERRITE CORE

Reading	Without	With	Threshold (UMBRAL)
0	3000	4100	3500
1	3066	4033	3500
2	3133	4000	3500
3	3100	3900	3500
4	3100	3800	3500
5	3000	3966	3500
6	3000	3933	3500
7	2966	3866	3500
8	3100	3966	3500
9	3100	3866	3500
10	3133	3766	3500

whether or not it contains ferrite inside. This strategy simplifies the detection process by translating the analog variation into a digital signal interpretable by the control system.

#### B. Prototype of three coils

After experimentally confirming that the ferrite-induced potential change can be digitally detected through the ADC, a more advanced version of the prototype was developed as shown in Fig.7 [14]. The objective was to extend the measurement capability by implementing a new design including three independent coils. This new setup would allow not only to validate the phenomenon under different spatial configurations, but also to evaluate the sensitivity of the system to variations in the position of the core within each coil. the prototype is shown in Fig.8 [14]

The behavior of the system under reference conditions can be seen in TableII, where all coils operate with air core. The readings of channels A0, A1 and A2 remain close to zero, with slight variations between  $\pm 10$  bits. This stable response indicates that, in the absence of ferrite, the circuit is in a neutral state with no significant disturbances. These data serve as a baseline to compare the point effect of inserting ferrite in each of the coils.



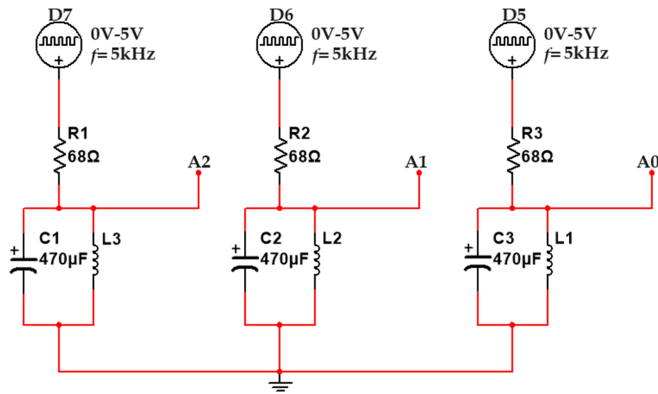


Fig. 7. Equivalent circuit of the RLC-03 prototype.

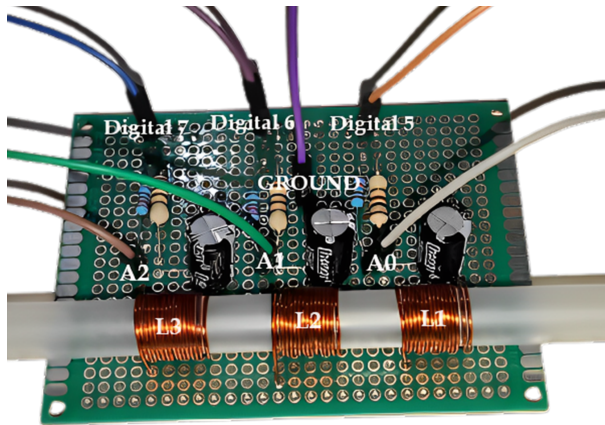


Fig. 8. RLC-03 prototype with air core in the coil and its connection to the ATmega.

TABLE II  
ADC BIT READINGS FROM 3 AIR-CORE COILS

Reading	A0	A1	A2
1	2	-7	0
2	-1	-12	-1
3	-2	-9	12
4	3	-9	7
5	5	-4	10
6	4	-6	9
7	8	-5	10
8	5	-8	8
9	9	-3	10
10	6	-9	10

By inserting a ferrite core in coil L1, a significant increase in the values recorded by channel A0 is evident, as shown in TableIII. The readings range from 12 to 18 bits, while A1 and A2 remain stable. This pattern demonstrates that the system responds in a localized manner to the change in reactance of a single coil, without generating interference in the others. The observed behavior validates the sensitivity of the system and its ability to identify the channel affected by the presence of ferrite.

The shift of the core towards coil L2 results in a new

TABLE III  
ADC BIT READINGS FROM A0 WITH FERRITE CORE IN L1

Reading	A0	A1	A2
1	18	-13	-2
2	13	-15	-2
3	18	-13	0
4	16	-12	1
5	17	-15	-2
6	18	-15	2
7	17	-12	0
8	16	-14	2
9	17	-15	1
10	12	-13	1

behavioral change, now in channel A1. As shown in TableIV, this channel shows high readings - with peaks close to 15 bits - while A0 and A2 retain values typical of the resting state. This condition confirms the functional independence between the coils and reinforces the reliability of the system to detect individual variations without ambiguity.

TABLE IV  
ADC BIT READINGS FROM A1 WITH FERRITE CORE IN L2

Reading	A0	A1	A2
1	6	15	11
2	5	13	11
3	5	10	6
4	5	12	8
5	9	11	8
6	8	11	8
7	5	11	8
8	7	9	9
9	7	11	9
10	9	11	11

In TableV ferrite is introduced in coil L3, generating a considerable increase in channel A2, with registers reaching up to 22 bits. This result corroborates the operating principle of the RLC-01 prototype: each channel responds only to the inductive variations caused by the ferrite in its own coil. A0 and A1 remain stable, which reinforces the isolation hypothesis and allows the system to be extrapolated to vertical level detection schemes.

TABLE V  
ADC BIT READINGS FROM A2 WITH FERRITE CORE IN L3.

Reading	A0	A1	A2
1	-1	-8	19
2	-4	-11	15
3	0	-7	16
4	0	-9	15
5	2	-11	20
6	1	-11	17
7	6	-11	20
8	3	-8	19
9	5	-11	22
10	2	-13	21

It is evidenced that the presence of the ferrite core affects exclusively the coil in which it is inserted, while the others maintain their readings within the usual range, without significant alterations. This confirms that the voltage variation



is localized and that the system is able to detect precisely in which coil the ferrite is located, without inter-channel interference.

The Moore machine process diagram of the code for the sea level measurement prototype is shown in Fig.10 [14].



Fig. 9. Moore State Machine Symbolology.

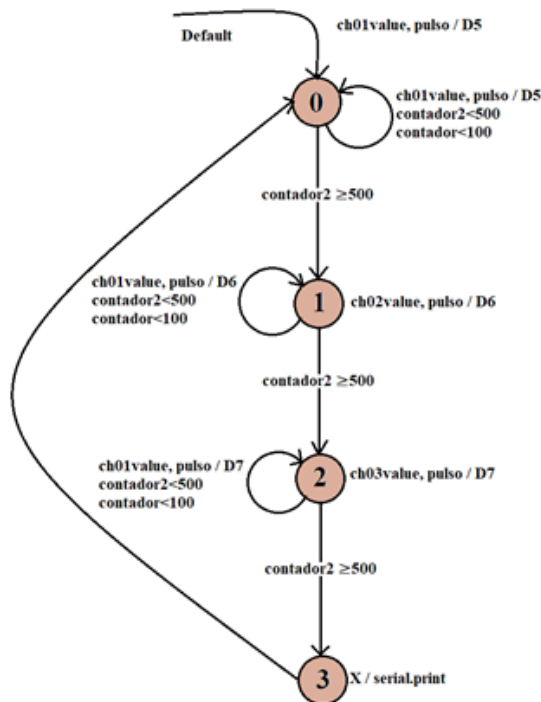


Fig. 10. Moore state machine built and tested for three RLC channels.

#### IV. CONCLUSIONS

The experimental data obtained validate the performance of the RLC-03 prototype as an inductive detection system based on local reactance variations caused by the presence of ferrite cores. Through multiple tests with three independent coils and dedicated analog inputs, it was demonstrated that the system is able to accurately identify which of the coils has been affected, without inter-channel interference. This clear and localized response evidences not only the adequate sensitivity of the ATmega microcontroller's ADC, but also the technical feasibility of using this approach to represent discrete levels of simulated height as part of a conceptual model for wave energy detection. A fundamental aspect in the efficiency of the system was the implementation of a Moore state machine, which allowed to sequentially control the activation of each of the

coils. This control scheme guarantees an orderly and rational use of the microcontroller resources, avoiding overlapping readings and reducing unnecessary energy consumption. The logic developed in the state machine acts as the coordination core of the system, precisely defining the activation, sampling and reading cycles of each analog channel. Thanks to this approach, it was possible to maximize ATmega performance and maintain stable operation even under varying load conditions.

Overall, the results support the effectiveness of the RLC-03 prototype design both electronically and logically, and lay the groundwork for its evolution into more complex marine sensing and monitoring systems. The use of state machine based architecture not only orders the internal operation of the system, but also opens the door to its future scalability, facilitating the incorporation of more sensors or reading levels without compromising the stability of the prototype. Finally, this research presents a functional methodology for the construction of a nonlinear equivalent electrical model, useful for the design and analysis of wave energy systems. The proposed model integrates an effective interface for transient analysis and long-term evaluation of system performance, facilitating tuning, optimization of key parameters and validation of new designs in marine renewable technologies.

#### ACKNOWLEDGMENT

#### REFERENCES

- [1] C. E. para América Latina y el Caribe (CEPAL), *El cambio climático y la energía en América Latina y el Caribe: una contribución al debate regional*. Santiago: Naciones Unidas, 2015, [En línea]. Disponible en: [https://repositorio.cepal.org/bitstream/handle/11362/39751/S1501198\\_es.pdf](https://repositorio.cepal.org/bitstream/handle/11362/39751/S1501198_es.pdf).
- [2] O. P. de la Salud, *Contaminación del aire en América Latina: desafíos y perspectivas*. OPS, 2020, [En línea]. Disponible en: <https://fi-admin.bvsalud.org/document/view/y2xxt>.
- [3] D. A. Sánchez and R. Martínez, "Estimación del recurso energético de oleaje en la costa caribeña hondureña," *Ingeniería y Desarrollo*, vol. 38, no. 1, pp. 98–112, 2020, [En línea]. Disponible en: <https://manglar.uninorte.edu.co/bitstream/handle/10584/11389/1124012630.pdf>.
- [4] M. Zamora, J. Gutiérrez, and E. Rivas, "Potencial energético undimotriz en nodos costeros de México. parte 1: Estimación energética," *Revista Energía y Ambiente*, vol. 6, no. 2, pp. 12–24, 2017, [En línea]. Disponible en: <https://www.researchgate.net/publication/321285397>.
- [5] B. I. de Desarrollo, *Watts on: Una mirada al sector energético de América Latina y el Caribe*. BID, 2021, [En línea]. Disponible en: <https://publications.iadb.org/publications/spanish/document/Watts-on-una-mirada-al-sector-energetico-de-America-Latina-y-el-Caribe.pdf>.
- [6] M. T. Pontes and R. D. Aguiar, "Limitaciones tecnológicas para la medición de energía undimotriz en zonas tropicales," *Revista de Energía Renovable Marina*, vol. 3, no. 1, pp. 21–29, 2012.
- [7] A. F. de O. Falcão, "Wave energy utilization: A review of the technologies," *Renewable and Sustainable Energy Reviews*, vol. 14, no. 3, pp. 899–918, 2010.
- [8] G. Salter, "Development of the duck wave energy converter," *Philosophical Transactions of the Royal Society A*, vol. 370, no. 1959, pp. 365–380, 2006.
- [9] M. Fernández and J. Ugarte, "Diseño de prototipos para energías marinas en contextos de bajo presupuesto," *Revista I+D Energía*, vol. 10, no. 3, pp. 115–130, 2021.
- [10] T. F. Bogart, J. A. Baltazar, and M. E. Ricchiuti, *Electrónica: Dispositivos y circuitos*, 6th ed. México: Pearson Educación, 2004.
- [11] J. W. Nilsson and S. A. Riedel, *Electric Circuits*, 11th ed. Boston: Pearson, 2019.
- [12] D. Halliday, R. Resnick, and J. Walker, *Fundamentals of Physics*, 10th ed. Hoboken: Wiley, 2014.



4

- [13] R. A. Serway and J. W. Jewett, *Physics for Scientists and Engineers with Modern Physics*, 10th ed. Boston: Cengage Learning, 2018.
- [14] C. Acosta and A. Carranza, "Author-generated image as part of the experimental development of the prototype," Author's original work, 2025, unpublished image.